

Numerical Analysis of Sleeve Monopole in Parallel-Plate Waveguide

Zhi Ning Chen,¹ Kazuhiro Hirasawa,² Ke Wu³

¹ Center for Wireless Communications, National University of Singapore, Singapore

² Institute of Information Sciences and Electronics, University of Tsukuba, Japan

³ Poly-Grames Research Center, Ecole Polytechnique, Montreal, Canada

Received 24 October 2000; revised 23 November 2000

ABSTRACT: A monopole with double sleeves, which consists of a resonant loading and a conventional sleeve monopole, is experimentally investigated. The loaded monopole is put vertically in a parallel-plate waveguide and driven by a coaxial feeder. The new structure exhibits a remarkably broad impedance bandwidth. In this paper, a modal expansion technique is used to numerically evaluate the impedance characteristics of the monopole by modeling the fields between the plates using cylindrical harmonic functions. A Fourier least-square integration is applied to finding the expansion coefficients by the boundary and continuity conditions. Prior to modeling the proposed sleeve monopole, the developed analysis scheme is examined for its convergence and accuracy. Calculated results are validated by the measurements. For the optimum design at 5.8 GHz, we investigate the effects of the structure parameters on the impedance characteristics. © 2001 John Wiley & Sons, Inc. *Int J RF and Microwave CAE* 11: 86–98, 2001.

Keywords: eigenmode expansion method; parallel-plate waveguide; sleeve monopole; waveguide transition; broadband design

I. INTRODUCTION

Due to their merits, such as geometrical simplicity and cost-effectiveness, the coaxially fed monopoles have been widely used in a large variety of microwave devices and communication antennas. Basically, a monopole can provide a reasonably good impedance match between a coaxial line and a parallel-plate waveguide over a certain frequency range. In this regard, a monopole may be used as either an adapter or a feeder to a waveguide, and this engineering application has been studied for a number of years [1–12].

As an adapter, the coaxially fed monopole transfers the power from a coaxial line to other

transmission line systems such as rectangular or parallel-plate waveguides [6–12]. As a feeder, the monopole is used as an antenna feeding network or a radial signal dividing–combining network of power amplifiers. Typically, it has been used in the design of direct broadcast satellite (DBS) planar receiving antennas and modified to satisfy some special needs in the designs [13–17]. It is also used in the designs of omnidirectional antennas or arrays in the communication systems. Usually, a linear monopole in its basic form suffers from a very limited impedance bandwidth. Thus, various loading techniques were proposed to enhance the bandwidth performance, including dielectric coatings [18], attached dielectric resonators [19–21], and disc-ended or top-hat structures [2, 9, 22, 23]. Alternative schemes have been developed on the basis of leaky-mode aperture-coupled dielectric resonators [24, 25] or radiating

Correspondence to: Zhi Ning Chen; e-mail: chenzn@cwc.nus.edu.sg.

Contract grant sponsor: Monbusho's grant-in-aid for Japan Society for the Promotion of Science (JSPS) Fellow Programs.

dielectric resonators [26]. More recently, a type of sleeve monopole integrated into a parallel-plate waveguide has been proposed to enlarge the impedance bandwidth, and this monopole comprises a resonant loading and a conventional sleeve geometry vertically located in a parallel-plate waveguide [27, 28].

Basically, the sleeve monopole is a modified version of a simple monopole with an extended outer conductor of the coaxial line by about a quarter axial wavelength of the line. The extended outer conductor is grounded and the cylindrical aperture operates as a radiator, whose maximum radiation is normal to the axis of the stem. It may be easy to obtain a good match between the monopole and coaxial line by adequately adjusting the sleeve length. Nevertheless, the sleeve monopole, similar to a linear monopole antenna, may have a broad bandwidth only for radiation pattern and not for input impedance [29]. It is difficult to overcome this inherent limitation resulting from a frequency-sensitive geometry. To remedy this problem, a second sleeve as a resonant loading has been used, coaxially located at the top of a conventional sleeve monopole. The additional sleeve generates parasitic resonance that can be used to tune and to broaden the impedance bandwidth. Therefore, a remarkably broad impedance bandwidth has been readily achieved by carefully designing the sleeve lengths. This performance has been improved without deteriorating other electrical characteristics. This structure also maintains the technical merits of a conventional monopole such as low cost and easy realizability with high modal purity.

A modal expansion technique similar to [23, 30–33] was extended to investigate the sleeve monopole. Geometrical parameters are rigorously considered in the model. These include end effects of the monopole, finite thickness of the sleeves, and dielectric jacket of the connector (for example, a commercial surface mount adapter (SMA) can be modeled). To begin with, the region of interest between the parallel plates is divided into four subregions. Electric and magnetic field components are formulated for each of the four subregions subject to the boundary conditions. Application of the boundary and continuity conditions for the field equations determines the expansion coefficients via a Fourier least-square integration. Subsequently, the fields in the parallel plates and the induced currents on the monopole can be calculated. Therefore, the criti-

cal design parameters such as input impedance and return loss can be obtained numerically. This analysis is validated by comparing results reported in [30] as well as our own experiments for a 5.8 GHz ISM-band (industrial, scientific, and medical) design. On the ground of the 5.8 GHz ISM design, we numerically conducted the parametric study on the impedance characteristics of the sleeve monopole.

II. THEORY AND FORMULATION

The configuration of the 5.8 GHz ISM design and a cylindrical coordinate system (ρ, ϕ, z) are shown in Figure 1. The optimized dimensions for the design are given here. The spacing of the parallel plates is h ($= 47$ mm) and the length of the inner cylindrical conductor l ($= 21.9$ mm). The radii of the probe and the dielectric jacket are denoted by r ($= 2.057$ mm) and a ($= 0.635$ mm), respectively. b ($= 11.8$ mm) and w ($= 17.0$ mm) stand for the lengths of two metallic sleeves while t ($= 0.28$ mm) is the thickness of the two sleeves. The whole structure is partitioned into four subregions marked by dielectric constants ϵ_n with $n = 1, 2, 3, 4$ ($\epsilon_n = \epsilon_{rn} \epsilon_0$), where $\epsilon_{r1} = \epsilon_{r3} = \epsilon_{r4} = 1.0$ and $\epsilon_{r2} = 2.08$. A small source region having its height d is designated with uniform electric field and its constant voltage source is V_0 . Similar to the analytical procedure in [30], a modal expansion technique is developed to formulate the structure. This procedure is recapitulated and essential field equations are derived for the sake of convenience.

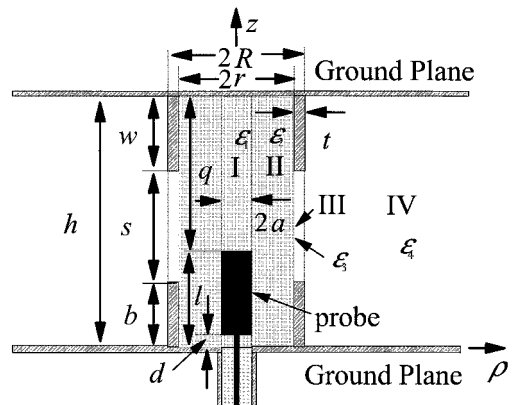


Figure 1. Geometrical description and physical notation of the proposed double-sleeve monopole housed in a parallel-plate waveguide.

A. Field Formulation

The four subregions of interest are in fact bounded by three cylindrical surfaces, namely, $\rho = a, r$, and R , respectively. Electric and magnetic fields in each subregion can be formulated in terms of an electric type (TM^z) Hertz potential [32]. The ground plates, the top of the monopole, and the ends of two sleeves are subject to the perfect electric conducting (PEC) condition. Finite-series or truncated modal field expansions are developed as follows by considering the boundary conditions.

Within subregion I ($\rho \leq a$ and $l \leq z \leq h$) above the top of the stem, we have

$$E_z^I(\rho, z) = \frac{1}{j\omega\epsilon_{r1}\epsilon_0\mu_0} \sum_{n=0}^{N_1} a_{1n} k_{\rho 1n}^2 J_0(k_{\rho 1n} \rho) \times \cos\left[\frac{n\pi}{q}(z-l)\right], \quad (1)$$

$$H_\phi^I(\rho, z) = \frac{1}{\mu_0} \sum_{n=0}^{N_1} a_{1n} k_{\rho 1n} J_1(k_{\rho 1n} \rho) \times \cos\left[\frac{n\pi}{q}(z-l)\right],$$

in which $k_1^2 = \epsilon_{r1}k_0^2$, $k_0^2 = \omega^2\epsilon_0\mu_0$, $q = h - l$, and

$$k_{\rho 1n} = \pm \sqrt{k_1^2 - (n\pi/q)^2} = \begin{cases} \sqrt{k_1^2 - (n\pi/q)^2} & k_1 \geq (n\pi/q), \\ -j\sqrt{(n\pi/q)^2 - k_1^2} & k_1 \leq (n\pi/q). \end{cases}$$

Inside subregion II (dielectric jacket) with $r \geq \rho \geq a$ and $0 \leq z \leq h$, the fields are given by

$$E_z^{II}(\rho, z) = \frac{1}{j\omega\epsilon_{r2}\epsilon_0\mu_0} \sum_{n=0}^{N_2} k_{\rho 2n}^2 \times [a_{2n}J_0(k_{\rho 2n}\rho) + b_{2n}N_0(k_{\rho 2n}\rho)] \times \cos\left(\frac{n\pi}{h}z\right), \quad (2)$$

$$H_\phi^{II}(\rho, z) = \frac{1}{\mu_0} \sum_{n=0}^{N_2} k_{\rho 2n} \times [a_{2n}J_1(k_{\rho 2n}\rho) + b_{2n}N_1(k_{\rho 2n}\rho)] \times \cos\left(\frac{n\pi}{h}z\right),$$

with $k_2^2 = \epsilon_{r2}k_0^2$ and

$$k_{\rho 2n} = \pm \sqrt{k_2^2 - (n\pi/h)^2} = \begin{cases} \sqrt{k_2^2 - (n\pi/h)^2} & k_2 \geq (n\pi/h), \\ -j\sqrt{(n\pi/h)^2 - k_2^2} & k_2 \leq (n\pi/h). \end{cases}$$

Over the aperture of the sleeve (region III) with $r \leq \rho \leq R$ and $b \leq z \leq (b+s)$, the fields are

$$E_z^{III}(\rho, z) = \frac{1}{j\omega\epsilon_{r3}\epsilon_0\mu_0} \sum_{n=0}^{N_3} k_{\rho 3n}^2 \times [a_{3n}J_0(k_{\rho 3n}\rho) + b_{3n}N_0(k_{\rho 3n}\rho)] \times \cos\left[\frac{n\pi}{s}(z-b)\right], \quad (3)$$

$$H_\phi^{III}(\rho, z) = \frac{1}{\mu_0} \sum_{n=0}^{N_3} k_{\rho 3n} \times [a_{3n}J_1(k_{\rho 3n}\rho) + b_{3n}N_1(k_{\rho 3n}\rho)] \times \cos\left[\frac{n\pi}{s}(z-b)\right],$$

where $k_3^2 = \epsilon_{r3}k_0^2$ and

$$k_{\rho 3n} = \pm \sqrt{k_3^2 - (n\pi/s)^2} = \begin{cases} \sqrt{k_3^2 - (n\pi/s)^2} & k_3 \geq (n\pi/s), \\ -j\sqrt{(n\pi/s)^2 - k_3^2} & k_3 \leq (n\pi/s). \end{cases}$$

The remaining radial unbounded subregion IV ($\rho \geq R$ and $0 \leq z \leq h$) is characterized by

$$E_z^{IV}(\rho, z) = \frac{1}{j\omega\epsilon_{r4}\epsilon_0\mu_0} \sum_{n=0}^{N_4} a_{4n} k_{\rho 4n}^2 H_0^{(2)}(k_{\rho 4n}\rho) \times \cos\left(\frac{n\pi}{h}z\right), \quad (4)$$

$$H_\phi^{IV}(\rho, z) = \frac{1}{\mu_0} \sum_{n=0}^{N_4} a_{4n} k_{\rho 4n} H_1^{(2)}(k_{\rho 4n}\rho) \times \cos\left(\frac{n\pi}{h}z\right),$$

with $k_4^2 = \varepsilon_{r4} k_0^2$ and

$$k_{\rho 4n} = \pm \sqrt{k_4^2 - (n\pi/h)^2}$$

$$= \begin{cases} \sqrt{k_4^2 - (n\pi/h)^2} & k_4 \geq (n\pi/h), \\ -j\sqrt{(n\pi/h)^2 - k_4^2}, & k_4 \leq (n\pi/h). \end{cases}$$

In the above equations, $J_m(\cdot)$, $N_m(\cdot)$, and $H_m^{(2)}(\cdot)$ are, respectively, Bessel functions of the first kind and the second kind, and Hankel function of the second kind, having the order $m = 0$ or 1.

B. Solutions for Coefficients of Field Expansions

To determine the coefficients of field expansions, the remaining boundary and continuity conditions in connection with the tangential fields should be fulfilled. Usual field Fourier matching technique is applied by integration over the boundaries and interfaces of the region. The procedure, in which the equations (A1)–(A4) for the unknown expansion coefficients are built up, is given in the Appendix.

Thus, combining the above linear equation eqs. (A1)–(A4) leads to a complex matrix system (5) of order $N_l = 2 \times N_2 + 2 \times N_3$, which is readily solved for the expansion coefficient a_{2n} , b_{2n} , a_{3n} , and b_{3n} . Then

$$\begin{bmatrix} [Z_{11}]_{N_2 \times N_2} & [Z_{12}]_{N_2 \times N_2} & [0]_{N_2 \times N_3} & [0]_{N_2 \times N_3} \\ [Z_{21}]_{N_3 \times N_2} & [Z_{22}]_{N_3 \times N_2} & [Z_{23}]_{N_3 \times N_3} & [Z_{24}]_{N_3 \times N_3} \\ [Z_{31}]_{N_2 \times N_2} & [Z_{32}]_{N_2 \times N_2} & [Z_{33}]_{N_2 \times N_3} & [Z_{34}]_{N_2 \times N_3} \\ [0]_{N_3 \times N_2} & [0]_{N_3 \times N_2} & [Z_{43}]_{N_3 \times N_3} & [Z_{44}]_{N_3 \times N_3} \end{bmatrix} \times \begin{bmatrix} [a_2]_{N_2 \times 1} \\ [b_2]_{N_2 \times 1} \\ [a_3]_{N_3 \times 1} \\ [b_3]_{N_3 \times 1} \end{bmatrix} = [V_0]_{N_l \times 1}. \quad (5)$$

C. Induced Currents on Monopole

Once the coefficients a_{2n} and b_{2n} become known, it can be straightforward to obtain the induced currents on the monopole through the relation-

ship $I(z) = 2\pi aJ = 2\pi aH_\phi^{\text{II}}(a, z)$, such that,

$$I(z) = 2\pi aH_\phi^{\text{II}}(a, z)$$

$$= \frac{2\pi a}{\mu_0} \sum_{n=0}^{N_2} k_{\rho 2n} [a_{2n} J_1(k_{\rho 2n} \rho) + b_{2n} N_1(k_{\rho 2n} \rho)] \cos\left(\frac{n\pi}{h} z\right). \quad (6)$$

In addition, the input impedance can readily be evaluated by using $Z_{\text{in}} = V_0/I(0)$ from eq. (6). Then, the return loss of the input coaxial line can directly be calculated.

The convergence of a numerical solution is normally related to a sufficient number of modes used in calculations. A good choice of the truncated numbers N_1 , N_2 , N_3 , and N_4 in our model closely depends on dimensions of the structure. As shown in Section IV, some criteria suggested in [30, 31] and convergence characteristics will be discussed with numerical calculations.

III. A 5.8 GHz ISM-BAND DESIGN

Some features of the proposed sleeve monopole structure will be shown with an engineering design for 5.8 GHz ISM-band applications. To begin with, a monopole structure is modeled numerically and its parameters are tuned back-and-forth and optimized such that a satisfactory impedance match is obtained at the operating frequency with a possible broad bandwidth. Subsequently, the monopole is designed and fabricated using an SMA connector with a long thin dielectric (Teflon) jacket and also a metallic tape sticking on a support (dielectric jacket). A coaxial line of 50 Ω is used as a feeder. Two electrically large circular conducting plates with diameters larger than $6\lambda_0$ are used to form an approximate radial parallel-plate waveguide. The lower sleeve is electrically connected to the bottom plate while the other is attached to the upper plate. The dielectric jacket is short-circuited at its ends by the plates.

Generally speaking, the structure can certainly be optimized for a particularly desired performance by adequately adjusting its parametric dimensions. In this design, a large impedance bandwidth with the possible best match characteristics at 5.8 GHz is expected. With the SMA connector, the design freedom remains in changing the size of the sleeves and the spacing between the parallel plates. Our simulation has shown the possibility of achieving the design goal. In fact, this

consideration also simplifies the design procedure. Some design rules and features will be suggested and discussed in Section IV on the basis of the parametric study.

IV. RESULTS AND DISCUSSION

A. Model Validation

Since the convergence is important for the technical merit of the modeling technique used in this work, a special discussion is made in this section. With reference to the criteria suggested in [30, 31], we carry out numerical experiments to assess the accuracy of the model and also to determine the adequate number of modal expansions.

In the following, only one of the four expansion numbers is changed while the others are fixed in accordance with the criteria [30, 31]. Figure 2 shows the calculated input impedance against those numbers. Compared with the experiments for N_2 and N_3 , N_1 , and N_4 -related results present a more rapid convergence. This is similar to what happens in the case of modeling a waveguide with a fin. To a large extent, it is because the modal solutions to Bessel's equations in subregion I or IV involve $J_m(k\rho)$ or $H_m^{(2)}(k\rho)$ for a real wave number k , respectively. In subregion II or III, modal behaviors, however, are described by a linear combination of $J_m(\cdot)$ and $N_m(\cdot)$ or $H_m^{(1)}(\cdot)$ and $H_m^{(2)}(\cdot)$. For an imaginary wave number k , they become the modified Bessel functions. This leads to a certain high-degree of complexity in the calculations. Potential numerical errors become nonnegligible and they may even exceed contributions from higher order modes. There-

fore, it is recommended to use a limited number of modes in the modeling although results are in principle more accurate with more modes. In other words, to have *enough* modes not only satisfies convergence requirements but also ensures an algorithmic stability with excellent accuracy. In our following calculations, a trade-off is considered between modeling accuracy and computational time. The number of expansion terms $N = 60$ or a little bit larger are used in this work. The CPU time at each frequency point is about 3 s on a PC Pentium III (700 MHz).

To validate our model, two examples, namely, a simple monopole ($w \rightarrow 0$, $b \rightarrow 0$, $\epsilon_{r,2} = 1.0$, and $h = 2.1\lambda_o$) and a conventional sleeve antenna ($w \rightarrow 0$, $\epsilon_{r,2} = 1.0$, $b = 0.25\lambda_o$, and $h = 2.1\lambda_o$) were selected for comparison of the experimental and modeling results given in [30, 31], respectively. Good agreements between them were found. Furthermore, a sleeve monopole at 5.8 GHz was designed and fabricated. The calculated and measured input impedances and return loss $|S_{11}|$ as shown in Figure 3 agreed quite well over 4–8 GHz.

It may sometimes be useful to use the input impedance together with the return loss $|S_{11}|$ even though the two parameters can be derived from each other. The input impedance shows the frequency response of impedance clearly, from which one can know the possible resonance. The return loss $|S_{11}|$ displays the matching condition directly, useful to the antenna design. Note that to simplify our reading of figures, from now on solid lines in the following figures are always used as "reference" or "standard," which has the optimized dimensions.

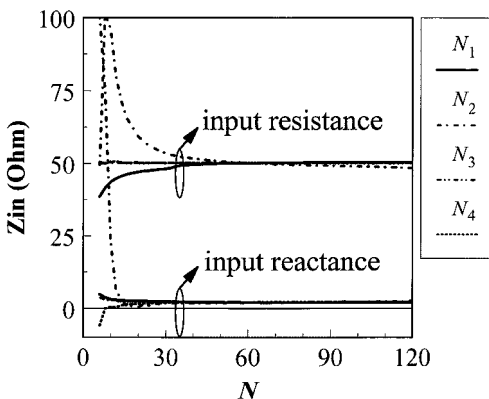
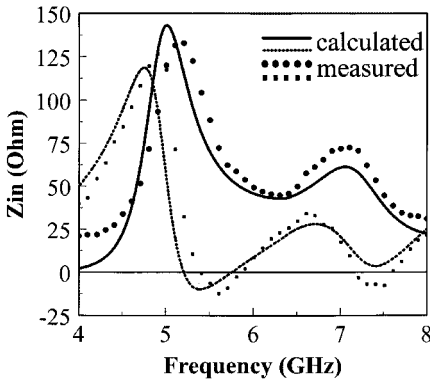


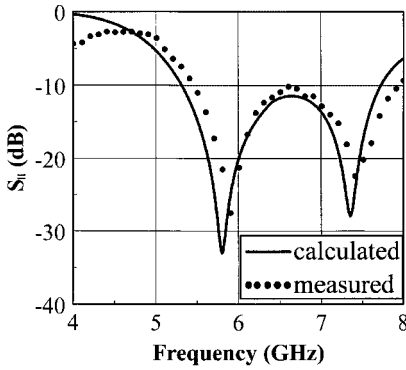
Figure 2. Convergence properties of the developed modal expansion algorithm in connection with the truncated numbers of modal expansion.

B. Design Results

A resonant frequency for parallel-type resonance is usually identified by a peak value of the input resistance. As can be seen from Figure 3(a), two parallel-type resonant frequencies f_{r1} ($= 5.02$ GHz) and f_{r2} ($= 7.06$ GHz) co-exist. Figure 3(b) shows that this structure provides a broad impedance bandwidth with a good match performance over a 5.32–7.72 GHz range (for $|S_{11}| \leq -10$ dB). In this design, the minimum point (-33.0 dB) of $|S_{11}|$ appears at 5.8 GHz. The second lowest point of $|S_{11}|$ (-27.9 dB) is located at 7.35 GHz. Within a 5.8–7.35 GHz range, $|S_{11}|$ is always lower than -11.4 dB at 6.63 GHz.



(a)



(b)

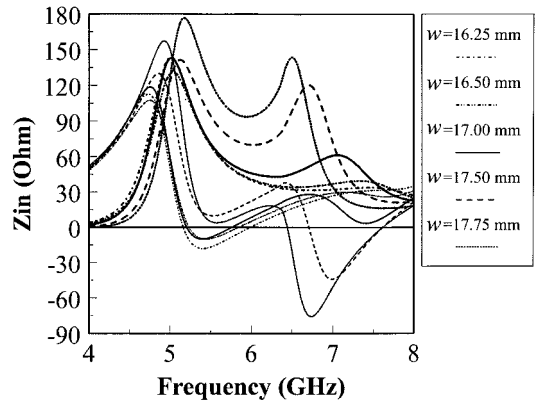
Figure 3. Comparison of calculated and measured results of our 5.8 GHz monopole example. (a) Input impedance Z_{in} ; and (b) return loss $|S_{11}|$.

Such a resonance behavior can simply be explained by circuit theory. It is known that there is a series-type resonance between the two parallel-type resonant frequencies. In our case, one parasitic parallel-type resonance is caused by a resonant loading, which occurs nearby the resonance due to the conventional sleeve monopole. Inductive reactance of the series-type resonance is effectively cancelled out by the capacitive reactance of the parasitic resonance when the latter moves close to the resonance at f_{r1} . Similarly, driving two neighboring parallel-type resonances closely leads to a partial cancellation of the reactance and then the resistance will be effectively increased, which takes place between the parallel-type resonance modes. This is why we can introduce a new mode near the operating mode or the shift of a neighboring mode adjacent to the operating mode in broadening the impedance bandwidth. It is also manifest that this proposed sleeve monopole operates within the range of $l/\lambda_o =$

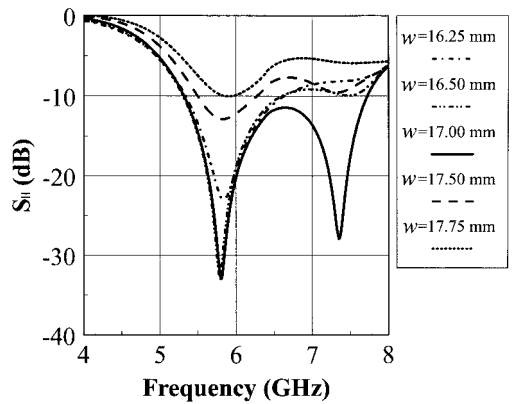
0.39 ~ 0.56 that differs from a quarter wavelength operating principle of the conventional monopole above the ground plane [34, 35]. With consideration of the dielectric coating effect ($\epsilon_{r2} = 2.08$ for Teflon), the approximate operating range of l/λ_d falls into 0.54 ~ 0.81.

C. Second Sleeve

As the second sleeve is the important element in this design, it is necessary to examine the effects of its parameters and spacing q on the characteristics of the monopole. Figure 4 shows the numerical results vs. frequency in the presence of the second sleeve with a different length w . Two interesting phenomena can be observed in Figure 4(a). First, the decrease of its length w from 17.0 to 16.25 mm hardly makes frequency f_{r1} vary but frequency f_{r2} shifts upward slightly and the



(a)



(b)

Figure 4. Calculated frequency responses of the proposed monopole for different length w of the second sleeve with (a) input impedance Z_{in} and (b) return loss $|S_{11}|$.

value of the second peak resistance $R_{\text{inmax}2}$ becomes small. Second, the extension of the second sleeve from 17.0 to 17.75 mm leads to a slight increase of the frequency f_{r1} while the frequency f_{r2} goes down and the peak value of $R_{\text{inmax}2}$ rises quickly, as opposed to the first scenario. It indicates the fact that the increase of the peak value of $R_{\text{inmax}2}$ stems from a high Q value of the resonant loading as the length w is extended. In the simulation, the spacing q is always fixed. In Figure 4(b), it is found that the influence of the length w on the impedance matching condition is significant. After checking Figure 4(a) and (b), it is reasonable to say that the first resonance is due to the conventional sleeve monopole and the second resonance is from the parasitic sleeve. Therefore, the second sleeve serves as not only a separate sleeve monopole-fed resonator with the resonant frequency f_{r2} but also a resonant loading of the sleeve monopole that affects the operating frequency f_{r1} . A modeling for a special case, namely, the monopole without the second sleeve, shows that the second resonance gradually disappears as the length w tends to be zero.

Figure 5 displays the frequency responses of the input impedance and $|S_{11}|$ as a function of the spacing q . It can be seen that increasing the spacing q pushes the frequency f_{r2} up, however, the frequency f_{r1} remains almost intact. Both of the resistance peak values increase for the small spacing q . The same reason as that for the length w is applied in this case. More precisely, the second parallel-type resonance is caused by the parasitic sleeve. On the other hand, increasing the spacing q results in a reduction in the ratio of the dielectric resonator radius to the height, which usually leads to the increases in resonant frequency. This implies that the size of the jacket and the length w significantly affect characteristics of the second sleeve, which can be considered as part of the dielectric jacket, indeed.

With the understanding of the role of the second sleeve in the structure, we are able to explain the effects of the radius r of the sleeve on the characteristics, as illustrated in Figure 6. In a similar way, one can find that the effects of the radius r on two resonance conditions are different. With reference to the first resonance, the input resistance quickly becomes large as the radius r increases from 1.81 to 2.21 mm, as plotted in Figure 6(a). Figure 6(b) also shows that the minimum of $|S_{11}|$ has a slight deviation from 5.8 GHz. As for the second resonance, the peak

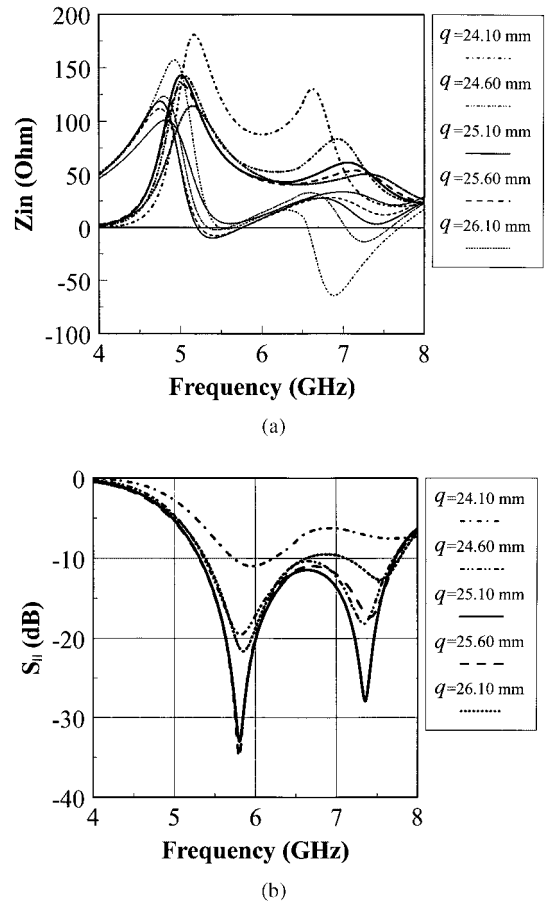
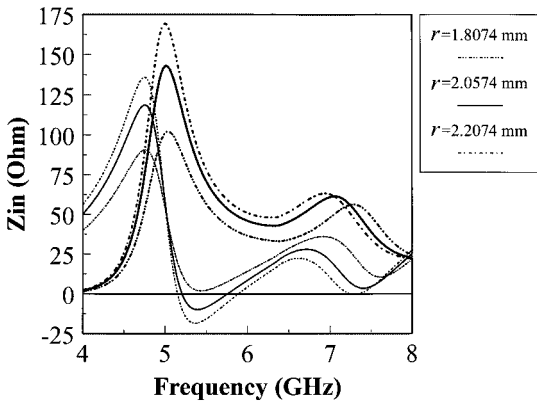


Figure 5. Calculated input impedance and return loss properties of the proposed monopole for different spacing q .

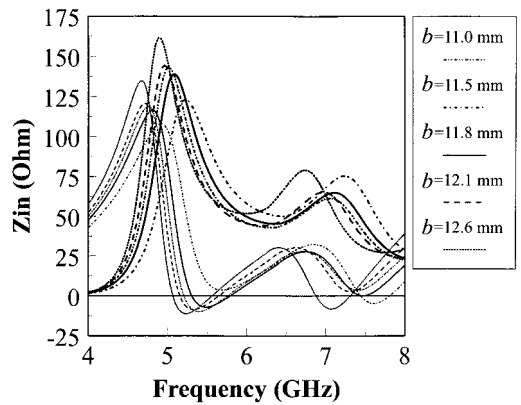
value of $R_{\text{inmax}2}$ changes a little bit whereas a different resonant frequency is generated for a different radius. It is not really surprising to see in Figure 6(b) that the impedance match performance can greatly be affected by choosing a different radius. This is because the increase of radius r implies the increase in the ratio of the dielectric resonator radius to the height as discussed above.

D. Other Parametric Effects

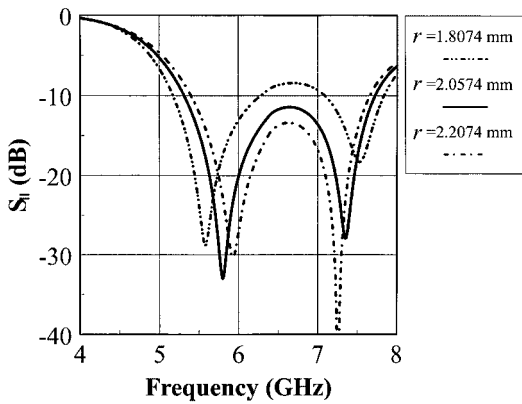
Now, let us take a close look at other parametric effects on the characteristics of the sleeve monopole. The frequency responses of the input impedance and $|S_{11}|$ are gathered in Figure 7 for a different sleeve length b . In fact, the effect of the length b on two resonant frequencies looks quite similar. Obviously, the shorter the length b is, the higher the resonant frequency becomes.



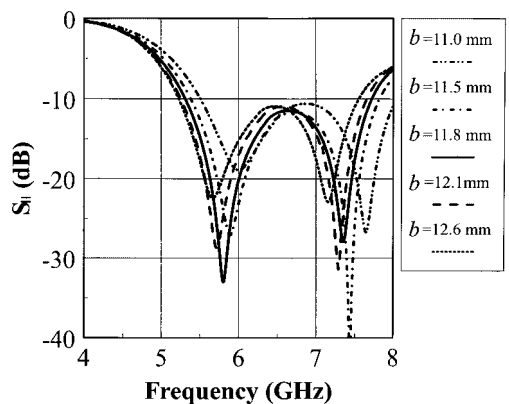
(a)



(a)



(b)



(b)

Figure 6. Parametric influence of the outer radius of the dielectric jacket r on the frequency response of the input impedance and return loss for the monopole example.

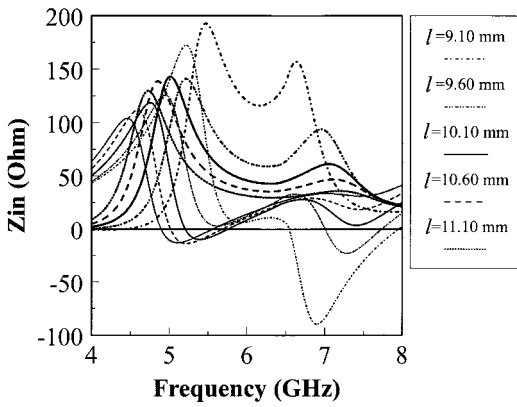
Figure 7. Input impedance and return loss characteristics of the monopole example vs. different lower sleeve length b .

From Figure 7(b), it is found that the expected matching condition is easily achieved by adjusting the length b . Similar to the conventional monopole radiating into the half free space, the monopole size in this work is still a key factor. Figure 8 displays the frequency-dependent curves as a function of the stub length $L (= l - b)$. Interestingly, the monopole manifests a similar behavior as the original and its impedance performance is improved using the resonant loading. Basically, the coupling between the loading and the monopole depends on the length L , especially with fixed spacing h and length w .

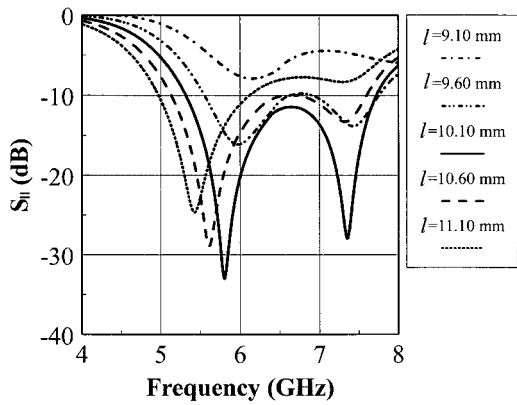
Figure 9 shows the impedance characteristics vs. the sleeve thickness t . It is seen that the thickness t has a slight impact on the input impedance. Nevertheless, a good impedance match can be achieved by adequately adjusting

the thickness t . As a matter of fact, a thin sleeve has a wider bandwidth as well as a better match than a thick sleeve. If the gap between two sleeves is considered as an aperture from which the monopole radiates into the parallel-plate waveguide, a thin sleeve is beneficial to increase the radiation efficiency [36, 37]. Therefore, a thin metal cover is always suggested in the design.

The calculated results related to the dielectric jackets with different dielectric constant ϵ_{r2} are shown in Figure 10. The strong effects of parameter ϵ_{r2} on the input impedance and $|S_{11}|$ are exhibited even though in a standard structure parameter ϵ_{r2} is around 2. In this analysis, the other dielectric constants 1.56 and 2.86 are taken into account. Figure 10(b) demonstrates how important an accurate characterization of the dielectric constants is. Judging from Figure 10(b), we may guess that the true relative dielectric

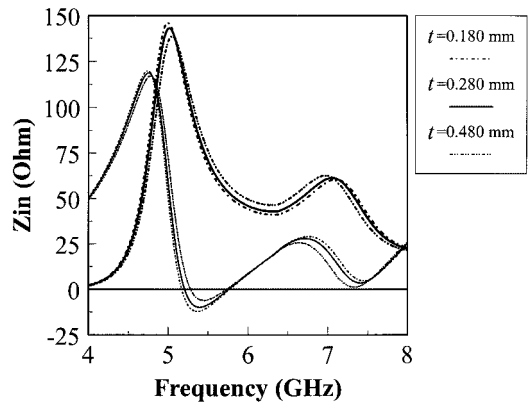


(a)

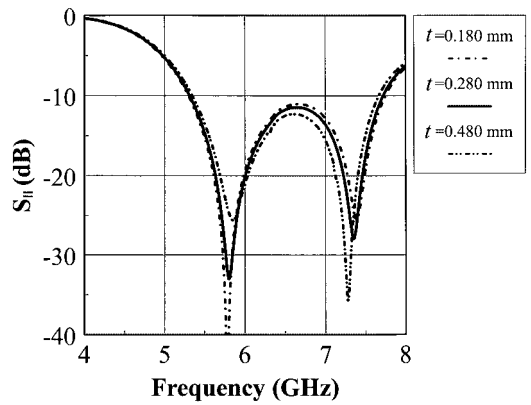


(b)

Figure 8. Calculated characteristics of the monopole example as a function of different probe length l .



(a)



(b)

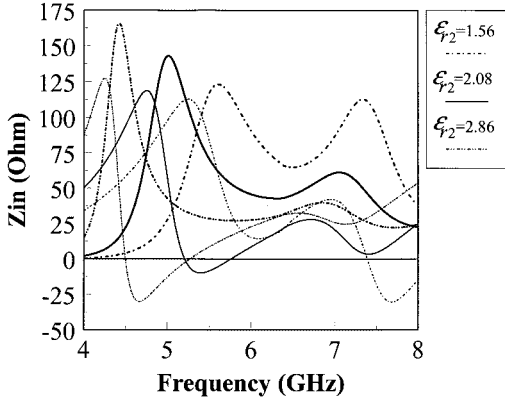
Figure 9. Frequency response behavior of the monopole example with different sleeve thickness t .

constant of the jacket in our prototype be slightly less than 2.08 used in the calculations. In this design, the dielectric jacket serves as not only a stem coating but also a resonant loading related to the second sleeve, which naturally yields a significant impact on the electrical characteristics of the sleeve monopole. In the case of a constant length w , the second resonance is nearly negligible as ϵ_{r2} is equal to 1. Eventually, the dielectric jacket can be effectively used to guide waves from the sleeve monopole to the second sleeve.

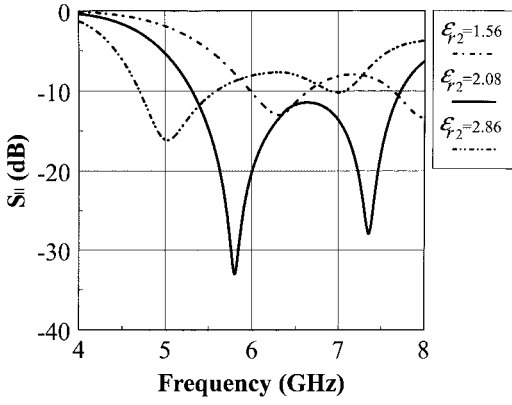
V. CONCLUSIONS

The characteristics of the double-sleeve monopole in a parallel-plate waveguide have been numeri-

cally analyzed using a modal expansion modeling technique. On the ground of a design example of 5.8 GHz ISM-band application, the parametrical study has been performed and the effects of the geometrical and electric parameters on the input impedance and bandwidth of the monopole have been examined. The study has demonstrated that the impedance performance of the monopole with the double-sleeve can be effectively improved by introducing the second sleeve operating as a parasitic resonant loading and strongly controlled by its geometrical and electric parameters. Moreover, with the attractive merits of remarkably broad bandwidth, simple structure, pure polarization, and low cost, the double-sleeve monopole has promising applications in the designs of broadband adapters and feeders for microwave circuits and antennas.



(a)



(b)

Figure 10. Curve plots of calculated input impedance and return loss for the monopole example with different dielectric constant ϵ_{r2} .

APPENDIX

At the interface of subregions I and II, the PEC condition for electric fields (on the surface of the monopole) and the continuity condition for both electric and magnetic fields (on the remaining aperture) should be satisfied. As for the source region, a uniform field was assumed, that is, $E_z^{\text{II}}(\rho, z) = -V_0/d$ for $0 \leq z \leq d$. Therefore, the following equation can be set up.

$$\sum_{n_2=0}^{N_2} a_{2n_2} \left[k_{\rho 2n_2} J_1(k_{\rho 2n_2} a) \right. \\ \times \sum_{n_1=0}^{N_1} \frac{k_{\rho 1n_1} J_0(k_{\rho 1n_1} a) T_{m,n_1}^{(2)} T_{n_2,n_1}^{(2)}}{\epsilon_{r1} J_1(k_{\rho 1n_1} a) I_{n_1 n_1}^{(4)}} \\ \left. - \frac{1}{\epsilon_{r2}} k_{\rho 2m}^2 J_0(k_{\rho 2m} a) I_{nm}^{(1)} \delta_{m,n_2} \right]$$

$$+ \sum_{n_2=0}^{N_2} b_{2n_2} \left[k_{\rho 2n_2} N_1(k_{\rho 2n_2} a) \right. \\ \times \sum_{n_1=0}^{N_1} \frac{k_{\rho 1n_1} J_0(k_{\rho 1n_1} a) T_{m,n_1}^{(2)} T_{n_2,n_1}^{(2)}}{\epsilon_{r1} J_1(k_{\rho 1n_1} a) I_{n_1 n_1}^{(4)}} \\ \left. - \frac{1}{\epsilon_{r2}} k_{\rho 2m}^2 N_0(k_{\rho 2m} a) I_{nm}^{(1)} \delta_{m,n_2} \right] \\ = j\omega \epsilon_0 \mu_0 \frac{V}{d} I_{nm}^{(3)}, \quad (\text{A1})$$

with

$$I_{nm}^{(3)} = \int_0^d \cos\left(\frac{m\pi}{h} z\right) dz \\ = \begin{cases} d & \text{for } m = 0, \\ \frac{h}{m\pi} \sin\left(\frac{m\pi d}{h}\right) & \text{for } m \neq 0, \end{cases} \\ T_{m,n}^{(2)} = \int_l^h \cos\left[\frac{n\pi}{q}(z-l)\right] \cos\left(\frac{m\pi}{h} z\right) dz \\ = \begin{cases} q & \text{for } m = n = 0, \\ \frac{m\pi}{h} & \\ (-1)^m \frac{h}{\left(\frac{m\pi}{h}\right)^2 - \left(\frac{n\pi}{q}\right)^2} \sin\left(\frac{m\pi q}{h}\right) & \\ \text{otherwise,} & \end{cases} \\ I_{nm}^{(4)} = \int_l^h \cos\left[\frac{n\pi}{q}(z-l)\right] \cos\left[\frac{m\pi}{q}(z-l)\right] dz \\ = \begin{cases} 0 & \text{for } m \neq n, \\ \int_l^h \cos^2\left[\frac{m\pi}{q}(z-l)\right] dz & \\ = \begin{cases} q & \text{for } m = n = 0, \\ q/2 & \text{for } m = n \neq 0. \end{cases} \end{cases}$$

Similarly, the remaining equations for calculating the expansion coefficients are derived. Over the interface of subregions II and III, they are given by

$$\frac{1}{\epsilon_{r2}} k_{\rho 2m}^2 [a_{2m} J_0(k_{\rho 2m} r) + b_{2m} N_0(k_{\rho 2m} r)] I_{nm}^{(1)} \\ = \frac{1}{\epsilon_{r3}} \sum_{n_3=0}^{N_3} k_{\rho 3n_3}^2 [a_{\rho 3n_3} J_0(k_{\rho 3n_3} r) \\ + b_{\rho 3n_3} N_0(k_{\rho 3n_3} r)] T_{m,n_3}^{(1)}, \quad (\text{A2})$$

$$\begin{aligned}
 & k_{\rho 3m} [a_{3m} J_1(k_{\rho 3m} r) + b_{3m} N_1(k_{\rho 3m} r)] I_{nm}^{(2)} \\
 &= \sum_{n_2=0}^{N_2} k_{\rho 2n_2} [a_{2n_2} J_1(k_{\rho 2n_2} r) \\
 &+ b_{2n_2} N_1(k_{\rho 2n_2} r)] T_{n,m}^{(1)}, \quad (A3)
 \end{aligned}$$

in which

$$\begin{aligned}
 I_{nm}^{(1)} &= \int_0^h \cos\left(\frac{n\pi}{h} z\right) \cos\left(\frac{m\pi}{h} z\right) dz \\
 &= \begin{cases} 0 & \text{for } m \neq n, \\ \int_0^h \cos^2\left(\frac{m\pi}{h} z\right) dz \\ = \begin{cases} h & \text{for } m = n = 0, \\ h/2 & \text{for } m = n \neq 0, \end{cases} \end{cases} \\
 T_{m,n}^{(1)} &= \int_b^{b+s} \cos\left[\frac{n\pi}{s}(z-b)\right] \cos\left(\frac{m\pi}{h} z\right) dz \\
 &= \begin{cases} s & \text{for } m = n = 0, \\ \frac{m\pi}{h} \\ \frac{\left(\frac{n\pi}{s}\right)^2 - \left(\frac{m\pi}{h}\right)^2}{\left(\frac{n\pi}{s}\right)^2 - \left(\frac{m\pi}{h}\right)^2} \\ \times \left[(-1)^{m+n} \sin\left(\frac{m\pi w}{h}\right) + \sin\left(\frac{m\pi b}{h}\right) \right] \\ \text{otherwise,} \end{cases} \\
 I_{mn}^{(2)} &= \int_b^{s+b} \cos\left[\frac{n\pi}{s}(z-b)\right] \cos\left[\frac{m\pi}{s}(z-b)\right] dz \\
 &= \begin{cases} 0 & \text{for } m \neq n, \\ \int_b^{s+b} \cos^2\left[\frac{m\pi}{s}(z-b)\right] dz \\ = \begin{cases} s & \text{for } m = n = 0, \\ s/2 & \text{for } m = n \neq 0. \end{cases} \end{cases}
 \end{aligned}$$

Over the interface of subregion III and IV, the characteristic equation is obtained as

$$\begin{aligned}
 & \sum_{n_3=0}^{N_3} a_{3n_3} \left\{ \frac{k_{\rho 3n_3}^2}{\epsilon_{r3}} J_0(k_{\rho 3m} R) \right. \\
 & \times \sum_{n_4=0}^{N_4} \frac{\epsilon_{r4} H_1^{(2)}(k_{\rho 4n_4} R) T_{n_4,m}^{(1)} T_{n_4,n_3}^{(1)}}{k_{\rho 4n_4} H_0^{(2)}(k_{\rho 4n_4} R) I_{n_4 n_4}^{(1)}} \\
 & \left. - k_{\rho 3m} J_1(k_{\rho 3m} R) I_{nm}^{(2)} \delta_{m,n_3} \right\}
 \end{aligned}$$

$$\begin{aligned}
 & + \sum_{n_3=0}^{N_3} b_{3n_3} \left\{ \frac{k_{\rho 3n_3}^2}{\epsilon_{r3}} N_0(k_{\rho 3m} R) \right. \\
 & \times \sum_{n_4=0}^{N_4} \frac{\epsilon_{r4} H_1^{(2)}(k_{\rho 4n_4} R) T_{n_4,m}^{(1)} T_{n_4,n_3}^{(1)}}{k_{\rho 4n_4} H_0^{(2)}(k_{\rho 4n_4} R) I_{n_4 n_4}^{(1)}} \\
 & \left. - k_{\rho 3m} N_1(k_{\rho 3m} R) I_{nm}^{(2)} \delta_{m,n_3} \right\} = 0, \quad (A4)
 \end{aligned}$$

REFERENCES

1. A.G. Williamson and D.V. Otto, Coaxial fed hollow monopole in a rectangular waveguide, *Electron Lett* 9 (1973), 218–220.
2. M.E. Bialkowski, Analysis of disc-type resonator mounts in parallel plate and rectangular waveguide, *AEÜ* 38 (1984), 306–310.
3. M.E. Bialkowski, Probe antenna in arbitrarily terminated rectangular waveguide, *AEÜ* 39 (1985), 190–192.
4. B. Tomasic and A. Hessel, Electric and magnetic current sources in the parallel plate waveguide, *IEEE Trans Antennas Propagat* AP-35 (1987), 1307–1310.
5. B. Tomasic and A. Hessel, Linear array of coaxially fed monopole elements in a parallel plate waveguide—Part I: Theory, *IEEE Trans Antennas Propagat* AP-36 (1988), 449–462.
6. B. Tomasic and A. Hessel, Linear array of coaxially fed monopole elements in a parallel plate waveguide—Part II: Experiment, *IEEE Trans Antennas Propagat* AP-36 (1988), 463–467.
7. J.M. Jarem, A method of moments and a finite-difference time-domain analysis of a probe-sleeve fed rectangular waveguide cavity, *IEEE Trans Microwave Theory Tech* MTT-39 (1991), 444–451.
8. R.B. Keam and A.G. Williamson, Analysis of a general coaxial-line/radial-line region junction, *IEEE Trans Microwave Theory Tech* MTT-41 (1993), 516–520.
9. M.E. Bialkowski, Analysis of a coaxial-to-waveguide adaptor including a descended probe and a tuning post, *IEEE Trans Microwave Theory Tech* MTT-43 (1995), 344–349.
10. M.E. Bialkowski, Modelling of a coaxial-to-waveguide power combining structure, *IEEE Trans Microwave Theory Tech* MTT-34 (1986), 937–942.
11. M.E. Bialkowski, Electromagnetic model of a planar radial-waveguide divider/combiner probes, *IEEE Trans Microwave Theory Tech* MTT-41 (1993), 1126–1134.
12. M.E. Bialkowski, Analysis of a coaxial-to-waveguide adaptor incorporating a dielectric coated probe, *IEEE Microwave Guided Wave Lett* 1 (1991), 211–214.
13. N. Goto and M. Yamamoto, Circularly polarized

- radial line slot antennas, IEICE Tech Rep AP-80-57 (1980), 43 (in Japanese).
14. M. Ando, T. Numata, J. Takada, and N. Goto, A linearly polarized radial line slot antenna, *IEEE Trans Antennas Propagat* AP-36 (1988), 1675–1680.
 15. P.W. Davis and M.E. Bialkowski, Experimental investigations into a linearly polarized radial slot antenna for DBS TV in Australia, *IEEE Trans Antennas Propagat* AP-45 (1997), 1123–1129.
 16. H. Sasazawa, Y. Oshide, K. Sakurai, M. Ando, and N. Goto, Slot coupling in a radial line slot antenna for 12-GHz band satellite TV reception, *IEEE Trans Antennas Propagat* AP-36 (1988), 1221–1225.
 17. M. Ando, S. Ito, S. Kawasaki, and N. Goto, A design of a radial line slot antenna with improved input VSWR, *IEICE Trans Commun* J70-B (1987), 495–504 (in Japanese).
 18. S.A. Long, M.W. Allister, and L.C. Shen, The resonant cylindrical dielectric cavity antenna, *IEEE Trans Antennas Propagat* AP-31 (1983), 406–412.
 19. A.A. Kishk, H.A. Auda, and B.C. Ahn, Radiation characteristics of cylindrical dielectric resonator antennas with new applications, *IEEE Antennas Propagat Newslett* (1989), 6–16.
 20. D.I. Kaklamani, C.N. Capsalis, and N.K. Uzunoglu, Radiation from a monopole antenna covered by a finite height dielectric cylinder, *Electromagnetics* 12 (1992), 185–216.
 21. Z.N. Chen, K.W. Leung, K.M. Luk, E.K.N. Yung, and K. Hirasawa, Characterization of probe-fed dielectric resonator between parallel grounded plates, *IEEE Antennas Propagat Symp*, Atlanta, Georgia, USA, June 1998, pp. 1730–1733.
 22. K.W. Leung, Z.N. Chen, K.M. Luk, and E.K.N. Yung, On the probe-fed dielectric resonator inside the parallel plate waveguide, *IEEE Trans Microwave Theory Tech* MTT-47 (1999), 1113–1117.
 23. M.A. Morgan and F.K. Schwing, Eigenmode analysis of dielectric loaded top-hat monopole antennas, *IEEE Trans Antennas Propagat* AP-42 (1994), 54–61.
 24. T. Wang, H. An, K. Wu, J.J. Laurin, and R.G. Bosiso, A novel leaky-mode cylindrical dielectric resonator used as feeds of omnidirectional antenna for wireless communications, *IEEE Microwave Theory Tech Symp*, Orlando, Florida, USA, 1995.
 25. H. An, T. Wang, R.G. Bosiso, and K. Wu, A cavity-restrained multi-stacked dielectric omnidirectional antenna for microwave and millimeter wave wireless communications, *Electron Lett* 30(25) (1994), 2086–2087.
 26. S. Qi and K. Wu, Leakage and resonance characteristics of radiating cylindrical dielectric structure suitable for use as a feeder for high-efficient omnidirectional/sectorial antenna, *IEEE Trans Microwave Theory Tech* 46 (1998), 1767–1773.
 27. Z.N. Chen, K. Hirasawa, and K. Wu, A novel sleeve antenna with broad bandwidth, *IEEE Antennas Propagat Symp*, Orlando, Florida, USA, July 1999, pp. 1244–1247.
 28. Z.N. Chen, K. Hirasawa, and K. Wu, A broadband monopole in a parallel plate waveguide, *Asia-Pacific Microwave Conf*, Singapore, December 1999, pp. 732–735.
 29. A.J. Poggio and P.E. Mayes, Pattern bandwidth optimization of the sleeve monopole antenna, *IEEE Trans Antennas Propagat* AP-14 (1966), 643–645.
 30. M.A. Morgan, R.C. Hurley, and F.K. Schwing, Computation of monopole antenna currents using cylindrical harmonics, *IEEE Trans Antennas Propagat* AP-38 (1990), 1130–1133.
 31. Z. Shen and R.H. MacPhile, Rigorous evaluation of the input impedance of a sleeve monopole by modal-expansion method, *IEEE Trans Antennas Propagat* AP-44 (1996), 1584–1591.
 32. R.F. Harrington, *Time-harmonic electromagnetic fields*, McGraw-Hill, New York, 1961.
 33. Z.N. Chen, K.W. Leung, K.M. Luk, and E.K.N. Yung, Evaluation of resonant frequency of a cylindrical probe-fed DR antenna, *Int J Electron* 84 (1998), 529–537.
 34. W.L. Stutzman and G.A. Thiele, *Antenna theory and design*, Wiley, New York, 1981.
 35. J.D. Kraus, *Antennas*, McGraw-Hill, New York, 1988.
 36. P.R. Haddad and D.M. Pozar, Characterization of aperture coupled microstrip patch antenna with thick ground plane, *Electron Lett* 30 (1994), 1106–1107.
 37. K.W. Leung, Z.N. Chen, K.M. Luk, and E.K.N. Yung, Aperture-coupled dielectric resonator antenna with a thick ground plane, *IEEE Trans Antennas Propagat* AP-46 (1998), 1242–1243.

BIOGRAPHIES

Zhi Ning Chen was born in Nanjing, People's Republic of China. He received his B.Eng., M.Eng., and Ph.D. in 1985, 1988, and 1993 all in electrical engineering, respectively. From 1988 to 1998, he was with the Institute of Communications Engineering, Southeast University, and City University of Hong Kong, respectively, as a Teaching Assistant, Lecturer, Associate Professor, Research Assistant, Research Associate,

Senior Research Associate, Research Fellow, and Postdoctoral Fellow, respectively. He was awarded Postdoctoral Fellowship (1997) and Invitation Fellowship (2001) from Japan Society for Promotion of Science (JSPS) in 1998 and conducted research at the University of Tsukuba, Japan. Currently, he is a Senior Member of Technical Staff in Centre for Wireless Communications, and is also managing the project

on research and development of antennas for mobile communications. His research interests involve in various kinds of communication antennas (including the modeling, design, and measurement of wire antennas, microstrip patch antennas, small antennas, and arrays) and computational electromagnetics and its applications. Since 1995, he has published more than 50 papers in international journals and conferences. In addition, he was also the author of more than 40 papers published in Chinese journals and conferences from 1987 to 1995.

Kazuhiro Hirasawa received his Ph.D. degree in Electrical Engineering from Syracuse University, Syracuse, NY, in 1971. From 1967 to 1975, he was with the department of Electrical and Computer Engineering, Syracuse University. From 1975 to 1977, he was a consultant on research and development of various antennas. Since 1978, he has been with the University of Tsukuba, Ibaraki, Japan. Currently, he is a Professor in the Institute of Information Science & Electronics. His research interests include cavity-backed slot antennas, circularly polarized wire antennas, mobile antennas, and adaptive arrays. He is co-author of *Small Antennas* (U.K.: Research Studies Press, 1987) and *Analysis, Design and Measurement of Small and Low-Profile Antennas* (in Japanese) (Tokyo, Japan: IEICE, 1996).

Ke Wu was born in Liyang, Jiangsu Province, People's Republic of China. He received the B.Sc. degree with distinction in radio engineering from Nanjing Institute of Technology (now Southeast University), Nanjing, People's Republic of China, in 1982 and the D.E.A. and the Ph.D. degree with distinction in optics, optoelectronics, and microwave engineering from the Institut National Polytechnique de Grenoble (INPG), France, in 1984 and 1987, respectively. He conducted research in the Laboratoire d'Electromagnetisme, Microondes et Optoelectronics (LEMO), Grenoble, France, prior to joining the Department of Electrical and Computer Engineering at the University of Victoria, B.C., Canada. Subsequently, he joined the Department of Electrical and Computer Engineering at the Ecole Polytechnique de Montreal (Faculty of Engineering at the University of Montreal) as an Assistant Professor, and he is now a full Professor. Dr. Wu held visiting or guest professorships at Telecom-Paris and INP-Grenoble, France, the City University of Hong Kong, the Swiss Federal Institute of Technology (ETH-Zurich), Switzerland, the National University of Singapore, the University of Ulm, Germany, as well as several short-term visiting professorships in many other universities. He also holds an honorary visiting professorship

of the Southeast University, China. He has been the head of the FCAR Research Group of Quebec on RF and millimeter-wave electronics and the director of the Poly-Grames Research Center, as well as the founding director of the newly developed Canadian Facility for Advanced Millimeter-wave Engineering (FAME). He has authored or co-authored over 270 referred journal and conference papers, and also several book chapters. His current research interests involve 3D hybrid monolithic planar and nonplanar integration techniques, active and passive circuits, antenna arrays, advanced field-theory based CAD and modeling techniques, and development of low-cost RF and millimeter-wave transceivers. He is also interested in the modeling and design of microwave photonic circuits and systems. He was Chairperson of the 1996 ANTEM's Publicity Committee and Vice-Chairperson of the Technical Program Committee (TPC) for the 1997 Asia-Pacific Microwave Conference (APMC'97). He has served on the FCAR Grant Selection Committee (1993–1996 and 1998–1999), and the TPC committee for the TELSIS and ISRAMT. He has also served on the ISRAMT International Advisory Committee. He was the general co-chair of the 1999 and 2000 SPIE's International Symposium on Terahertz and Gigahertz Electronics and Photonics that were held in Denver and San Diego, respectively. Dr. Wu received a U.R.S.I. Young Scientist Award, the Institute of Electrical Engineers (IEE) Oliver Lodge Premium Award, the Asia-Pacific Microwave Prize Award, the University Research Award "Prix Poly 1873 pour l'excellence en recherche" from the Ecole Polytechnique on the occasion of its 125th anniversary, and the Urgel-Archambault Prize (the highest honor) in the field of Physical Sciences, Mathematics, and Engineering from the French-Canadian Association for the Advancement of Science (ACFAS). He has served on the editorial or review boards of various technical journals, including *IEEE Transactions on Microwave Theory and Techniques*, *IEEE Transactions on Antennas and Propagation*, *IEEE Microwave and Guided-Wave Letters*, and *Microwave and Optical Technology Letters*. Dr. Wu served on the 1996 IEEE Admission and Advancement (A & A) Committee, the Steering Committee for the 1997 joint IEEE AP-S/URSI International Symposium. He has also served as a TPC member for the IEEE MTT-S International Microwave Symposium. He has been elected into the board of directors of Canadian Institute for Telecommunication Research (CITR). He serves on the Technical Advisory Board of Lumenon Lightwave Technology, Inc. Currently, Dr. Wu is the chair of the joint IEEE chapters of MTT-S/APS/LEOS in Montreal. He is a member of the Electromagnetics Academy. He received his IEEE Fellow Award in 2001.